


Acoustoelasticity analysis of shear waves for nonlinear biomechanical characterization of oil-gelatin phantoms

Conference Paper**Author(s):**

Chintada, Bhaskara R.; Rau, Richard; [Goksel, Orcun](#) 

Publication date:

2019

Permanent link:

<https://doi.org/10.3929/ethz-b-000370205>

Rights / license:

[In Copyright - Non-Commercial Use Permitted](#)

Originally published in:

<https://doi.org/10.1109/ULTSYM.2019.8925670>

Acoustoelasticity Analysis of Shear Waves for Nonlinear Biomechanical Characterization of Oil-Gelatin Phantoms

Bhaskara Rao Chintada, Richard Rau, Orcun Goksel
Computer-assisted Applications in Medicine, ETH Zurich, Switzerland

Abstract—Shear waves speed (SWS) has found use in staging the liver fibrosis; however, it has shown poor specificity in the early detection and staging of nonalcoholic fatty liver disease (NAFLD) and it is found that SWS may act as a confounding factor to that end, especially with fibrosis that typically coexist. Different tissue compositions exhibit varying nonlinear characteristics. The nonlinear relationship of shear modulus as a function of applied stress/strain can be deduced using acousto-elasticity analysis. In this work, we are studying nonlinear characteristics of two sets of oil-gelatin phantoms: one set of phantoms represent steatotic stages while the other set emulates additional biomechanical changes following the onset of fibrotic processes in the liver. We found that the nonlinear mechanical parameter we estimated, known as 'A', decreased from -16.9 kPa to -4.6 kPa with the progression of emulated steatosis, later increasing to -21.0 kPa with the emulation of fibrosis progression. The results from these in-vitro phantom experiments demonstrate the potential of using acousto-elastic analysis and non-linear characteristics of shear-wave travel as a biomarker in reducing the confounding effects of SWS for the early detection and staging of liver steatosis; with a model demonstrated to disentangle fibrotic and steatotic processes.

Index Terms—Ultrasound, Shear-wave elastography, Liver, Steatosis, Fibrosis

I. INTRODUCTION

It is a well known phenomenon that pathological changes in soft tissues lead to changes in biomechanical properties, which resulted in the development of numerous noninvasive imaging modalities to characterize tissue biomechanical properties. Ultrasound *shear-wave elastography* (SWE) is one of these techniques in which acoustic radiation force is used to induce shear waves. The induced shear waves are monitored by ultrafast ultrasound imaging to determine *shear wave speed* (SWS), which is directly related to the shear modulus of the targeted soft tissue [1]. This method is used in several clinical applications, such as the diagnosis and staging of liver fibrosis [2], [3]. However, it has shown poor specificity in the early-stage diagnosis of nonalcoholic fatty liver disease (NAFLD) [4] – a liver disease widespread around the world and that affects 30% of population in the United States [5]. NAFLD is characterized by histological changes ranging from simple, benign steatosis (abnormal retention of lipids in the cells) to *nonalcoholic steatohepatitis* (NASH). The late disease stage of NASH involves severe consequences such as fibrosis, cirrhosis, liver failure and eventually need for liver transplantation. When NAFLD is diagnosed at early stages,

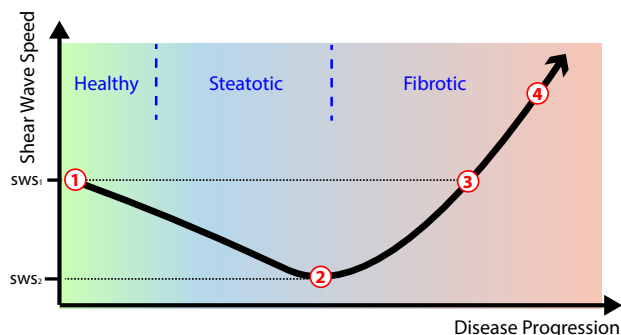


Fig. 1. Typical shear wave speed characteristics with liver disease progression. Shear wave speed (SWS) is first reduced due to fat accumulation, and then increased with the onset of fibrosis, which has a dominant effect in SWS. Stages relevant for our study are marked with respect to disease progression: ① healthy liver tissue, ② following steatotic processes and fat deposition, ③ SWS increase with the early fibrosis at the onset of NASH, ④ for late fibrotic stages leading to cirrhosis. For assessing disease progression, measuring SWS alone would thus be ambiguous for measurements between SWS_1 and SWS_2 .

the pathological processes may be treatable and reversible. The poor specificity of SWS in early diagnosis of NAFLD is mainly due to presence of steatosis, which may appear as a reduction in SWS due to increased fat content, acting as a confounder together with later fibrosis [6], as illustrated in Fig. 1. With adipose tissue accumulation during early steatosis “softening” the tissue, SWS in liver starts to decrease from a healthy state ①. At some steatotic state 2, the body triggers inflammatory responses [7], hence starting fibrotic pathological processes in the liver (i.e., NASH). Collagen build up during fibrosis increases the liver stiffness, thereby increasing the SWS, which at some point ③ would equal to and later ④ significantly surpass the healthy SWS range. Current SWS based diagnostic approaches and most research studies so far focus on such late-stage disease, i.e. ③-④.

To further understand the pathological changes in soft tissues, additional mechanical bio-markers obtained from shear-wave analysis could be useful, helping differentiation and resolving ambiguity especially during early disease progression (i.e. between ①-③ in Fig. 1). For instance, dispersion of SWS, which may be related to tissue viscosity, was shown in [8] to correlated with the degree of steatosis in oil-gelatin phantom experiments and a mouse liver model. Shear

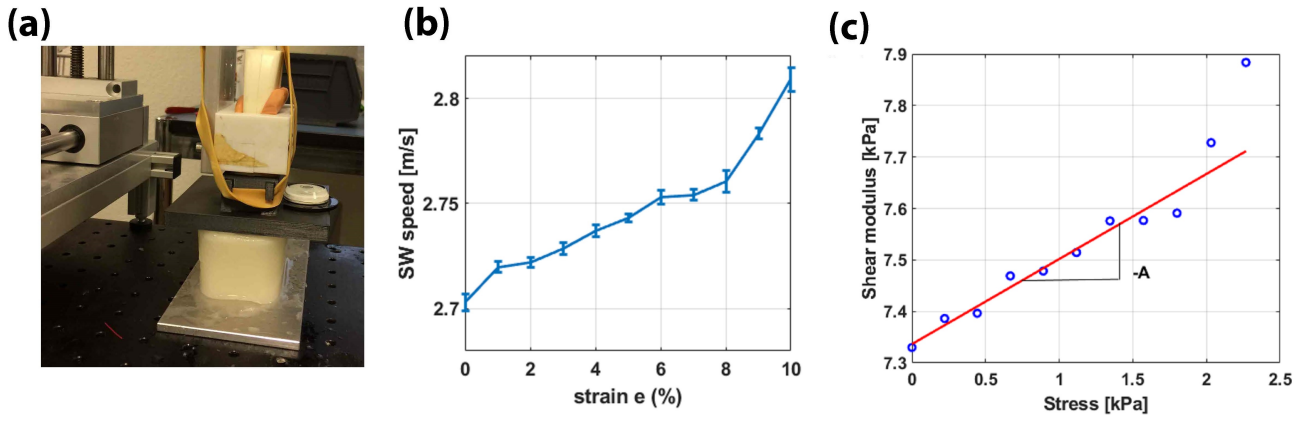


Fig. 2. Experimental setup and data processing steps of acousto-elasticity analysis (a) Experimental setup. (b) Shear wave speed of a phantom as a function of applied strain. (c) Stress, computed from uniaxial compression relationship (i.e., Eq.3) vs Shear modulus, derived from the relationship $\mu = \rho v^2$; a line is fitted to compute 3rd order non-linearity parameter A .

modulus non-linearity, which can be derived using acousto-elasticity (AE) analysis, can be another biomarker for differentiation. AE describes the dependence of SWS as a function of applied stress/compression, allowing to estimate non-linear biomechanical parameters [9]. Based on this phenomenon, several studies were conducted on porcine liver samples [10], [11], kidney samples [12], and brain tissue samples [13]. For porcine liver samples, frequency variations of non-linear mechanical parameters were also recently studied in [14].

Mechanical indentation experiments were used in [15] to study changes in elastic modulus with respect to applied strain, depending on tissue composition. It was found that elastic modulus in fat tissue is 10 times less sensitive to strain changes, compared to fibrous tissue. Therefore, with increased fat deposition during early NAFLD, we expect smaller changes in shear modulus across different levels of applied strain, compared to that at later NAFLD stages due to competing collagen deposition counteracting and reducing the relative effects from fat.

In this paper, we employ SWE using AE to study non-linear mechanical parameters of liver disease progression of NAFLD, with an oil-gelatin phantom model. Increasing steatotic stages are modelled with increased oil concentrations and the fibrotic effects by increased gelatin.

II. MATERIALS AND METHODS

A. Phantom preparation

To study the effects on the non-linear mechanical parameter with liver disease progression in NAFLD, we prepared 6 tissue mimicking phantoms {1..6} with different oil/gelatin concentrations. There were separated into two subsets. In the first subset (modeling steatosis), the oil content was gradually increased (castor oil 0%, 5%, 10%, and 15%) to mimic the increasing steatosis levels, while keeping the gelatin content constant (8%). The phantom with (0%) oil represents the healthy liver. For the second subset (modeling fibrosis), the collagen content was increased (gelatin 10% and 16%) to

mimic increasing fibrosis levels, while keeping the fat content constant (15%).

The phantoms were prepared following the procedure in [8]. We pre-heated distilled water to $\approx 70^\circ\text{C}$ before mixing in predetermined percentages of gelatin (G2500, Sigma-Aldrich chemical, USA) and castor oil (259853, Sigma-Aldrich chemical, USA). Anionic surfactant of concentration 4 cc/L was added to make oil droplets sufficiently small such that castor oil mixes homogeneously with gelatin. After the mixture is cooled down to $\approx 50^\circ\text{C}$, 1% of cellulose (S5504, Sigma-Aldrich chemical, USA) was added to provide scattering, essential for shear-wave tracking. The mixture was then let to cool down further and, while still in a semi-liquid state, was poured into a 100 mm \times 40 mm \times 50 mm mould. Until this point in time throughout the preparation processes, the mixture was stirred at a low speed in order to avoid oil separation from gelatin and to ensure a homogeneous scatterer distribution. The phantom mixtures were then refrigerated at 4°C for 18 h. Prior to data acquisition, the phantoms were removed from their moulds and kept at room temperature for 6 h for a uniform temperature distribution.

B. Data acquisition

To characterize the phantoms with different oil/gelatin compositions, we herein employ AE measurements based on acoustic radiation force induced shear waves, similarly to [14]. Shear waves are created using the supersonic shear-wave imaging technique [16], which generates a cylindrical shear wave with three subsequent high intensity pushes of 200 μs duration at three axially separated foci with a separation of 5 mm in depth. Shear-wave propagation is then tracked utilizing ultrafast ultrasound imaging at 10 k frames-per-second and coherent compounding of three angled plane waves at $(-8^\circ, 0^\circ, 8^\circ)$, using a 3rd order moving-average filter. This acquisition sequence was programmed in a research ultrasound machine (Verasonics, Seattle, WA, USA) for a 128-element linear-array transducer (Philips, ATL L7-4) operated at 5 MHz center frequency.

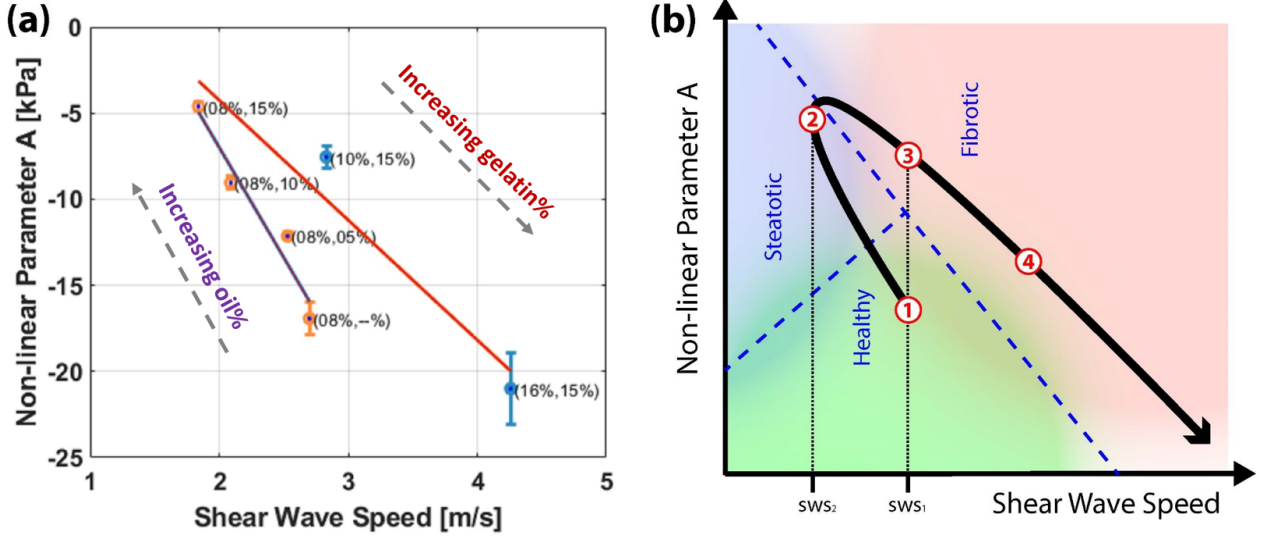


Fig. 3. The plots showing (a) 3rd order non-linear parameter A vs. shear-wave speed for various oil-gelatin phantoms. Two lines are fitted to phantoms #1–#4 and #4–#6, respectively, representing early steatotic and later fibrotic progression. (b) A model for non-linear parameter A and shear-wave speed relationship with liver disease progression, estimated from the experimental results. Numbered markers correspond to disease stages in Fig. 1.

C. Theory of acousto-elasticity

In this study we determine the mechanical parameters of the phantoms from measured SWS values as a function of applied uniaxial stress based on the theory of AE. The linear AE dependence of shear modulus on uniaxial stress can be derived using the equations of motion for elastic waves. Considering shear waves polarized along the axis of deformation, the following equation is obtained [9]:

$$\rho v^2 = \mu_0 - \sigma \frac{A}{12\mu_0} \quad (1)$$

with the tissue density ρ , the shear-wave speed v , the third-order elastic constant A , the applied stress σ , and the shear modulus μ_0 in a stress-free condition.

The apparent tangent shear modulus can be computed using $\mu = \rho v^2$ at each loading step i . Considering $\mu = \frac{1}{3} \frac{\partial \sigma}{\partial e}$ with an applied elongation ($e > 0$) or compression ($e < 0$), the apparent tangent shear modulus is then

$$3\mu_i = \frac{(\sigma_{i+1} - \sigma_i)}{(e_{i+1} - e_i)}. \quad (2)$$

Under uniaxial compression, apparent stress can be computed by

$$\sigma_{i+1} = \sigma_i + 3\mu_i(e_{i+1} - e_i) \quad (3)$$

with σ_0 being the stress at the initial unloaded state, which is considered herein to be close to 0 Pa when the probe is barely in contact with tissue, i.e. exerting minimal stress.

D. Experiments

Shear wave acousto-elasticity experiments were conducted by applying compressions in 0.5 mm steps up to 5 mm (corresponding to 1% increments up to 10% strain, given the height of our phantoms) using a motorized three-axis linear stage. An

TABLE I
MEASURED SWS AND 3RD ORDER NON-LINEAR PARAMETER
(\pm STANDARD DEVIATIONS) FOR THE PHANTOMS USED IN THIS STUDY

Phantom	Composition [Gelatin%, Oil%]	SWS [m/s]	A [kPa]
#1	8%, 0%	2.70 ± 0.01	-16.9 ± 0.9
#2	8%, 5%	2.53 ± 0.02	-12.1 ± 0.2
#3	8%, 10%	2.09 ± 0.01	-9.0 ± 0.4
#4	8%, 15%	1.84 ± 0.01	-4.6 ± 0.2
#5	10%, 15%	2.83 ± 0.01	-7.5 ± 0.6
#6	16%, 15%	4.26 ± 0.02	-21.0 ± 2.1

ultrasound probe, attached to this positioning stage, was used for both initiating shear-waves via acoustic radiation force and imaging the resulting shear waves. To provide uni-axial compression on phantoms, a compression plate of dimensions 100 mm \times 100 mm (with a small window for imaging through) was attached on the front of the ultrasound probe, as shown in Fig. 2a.

Particle velocity profiles of shear wave IQ data acquired at each compression step were tracked using the 2D Loupas autocorrelation method [17]. Next we computed SWS as the group velocity v_i at each compression step $i \in \{1..n\}$ using a robust 1D cross-correlation method [18].

Computed SWS values v_i above were then used in (1) to obtain the 3rd order non-linear parameter A from the slope of the apparent tangent shear modulus, as a function of applied stress, as exemplified in Fig. 2c.

III. RESULTS AND DISCUSSION

Relationship between SWS at stress-free state and 3rd order non-linear parameter A was shown in Fig. 3a for all the phantoms used in this study. It can be observed that, for phantoms (#1–#4) modeling increased steatotic stages,

SWS and magnitude of 3rd order non-linear parameter A are decreased, respectively, from 2.70 m/s to 1.84 m/s and -16.9 kPa to -4.6 kPa. For phantoms (#4–#6) modeling increasing fibrotic processes, SWS and the magnitude of A both increase again up to 4.26 m/s -21.0 kPa, respectively – but this time at different rates, potentially allowing for differentiating from the healthier stages. Measured SWS and 3rd order non-linear parameter 'A' for all the phantoms were summarized in Table I.

Given the experimental observations, Fig. 3b extends the SWS illustration in Fig. 1, by introducing a model for disease progression with the effect of different pathological processes, based on both SWS and non-linear parameter A. It is illustrated in Fig. 3b that the ambiguity of using SWS alone for quantifying early stage steatosis can be resolved by using a two-parameter model with the inclusion of non-linearity; i.e. although healthy ① and early-stage NASH ③ have the same SWS value, it may be possible to differentiate them based on the non-linearity parameter A.

Note that oil-gelatin phantoms used in this study are simple models of complex liver tissues and pathological processes. Though we anticipate a similar trend for non-linear parameter A with increasing steatosis and fibrosis, this should be studied in the future in in-vivo disease models, e.g. with respect to biopsy-proven liver samples.

In this study we have shown that measuring non-linear parameter using AE could be an additional bio-marker to detect the early stage of liver disease. However, due to anatomical complexity and constraints around the liver, it may not be straight-forward to apply uni-axial compression in-vivo while collecting shear wave data.

IV. CONCLUSIONS

In this work, we have studied the non-linear mechanical parameters of the disease progression of NAFLD with the help of oil-gelatin phantoms and the theory of acousto-elasticity. Results have revealed the feasibility of using 3rd order non-linear parameter along with shear wave velocity values in the early detection of NAFLD.

ACKNOWLEDGEMENTS

Funding provided by the Swiss National Science Foundation (SNSF), a Swiss Government Excellence Scholarship, and Promedica Foundation.

REFERENCES

[1] A. P. Sarvazyan, O. V. Rudenko, S. D. Swanson, J. B. Fowlkes, and S. Y. Emelianov, "Shear wave elasticity imaging: a new ultrasonic technology of medical diagnostics," *Ultrasound in medicine & biology*, vol. 24, no. 9, pp. 1419–1435, 1998.

[2] M. Friedrich-Rust, M.-F. Ong, S. Martens, C. Sarrazin, J. Bojunga, S. Zeuzem, and E. Herrmann, "Performance of transient elastography for the staging of liver fibrosis: a meta-analysis," *Gastroenterology*, vol. 134, no. 4, pp. 960–974, 2008.

[3] M. L. Palmeri, M. H. Wang, J. J. Dahl, K. D. Frinkley, and K. R. Nightingale, "Quantifying hepatic shear modulus in vivo using acoustic radiation force," *Ultrasound in medicine & biology*, vol. 34, no. 4, pp. 546–558, 2008.

[4] T. Poynard, M. Munteanu, E. Luckina, H. Perazzo, Y. Ngo, L. Royer, L. Fedchuk, F. Sattouf, R. Pais, P. Lebray *et al.*, "Liver fibrosis evaluation using real-time shear wave elastography: applicability and diagnostic performance using methods without a gold standard," *Journal of hepatology*, vol. 58, no. 5, pp. 928–935, 2013.

[5] J. D. Browning, L. S. Szczepaniak, R. Dobbins, P. Nuremberg, J. D. Horton, J. C. Cohen, S. M. Grundy, and H. H. Hobbs, "Prevalence of hepatic steatosis in an urban population in the united states: impact of ethnicity," *Hepatology*, vol. 40, no. 6, pp. 1387–1395, 2004.

[6] M. Yoneda, K. Suzuki, S. Kato, K. Fujita, Y. Nozaki, K. Hosono, S. Saito, and A. Nakajima, "Nonalcoholic fatty liver disease: Us-based acoustic radiation force impulse elastography," *Radiology*, vol. 256, no. 2, pp. 640–647, 2010.

[7] S. Ogawa, F. Moriyasu, K. Yoshida, H. Oshiro, M. Kojima, T. Sano, Y. Furuichi, Y. Kobayashi, I. Nakamura, and K. Sugimoto, "Relationship between liver tissue stiffness and histopathological findings analyzed by shear wave elastography and compression testing in rats with non-alcoholic steatohepatitis," *Journal of Medical Ultrasonics*, vol. 43, no. 3, pp. 355–360, 2016.

[8] C. T. Barry, B. Mills, Z. Hah, R. A. Mooney, C. K. Ryan, D. J. Rubens, and K. J. Parker, "Shear wave dispersion measures liver steatosis," *Ultrasound in Medicine & Biology*, vol. 38, no. 2, pp. 175–182, 2012.

[9] J.-L. Gennisson, M. Rénier, S. Catheline, C. Barrière, J. Bercoff, M. Tanter, and M. Fink, "Acoustoelasticity in soft solids: Assessment of the nonlinear shear modulus with the acoustic radiation force," *The Journal of the Acoustical Society of America*, vol. 122, no. 6, pp. 3211–3219, 2007.

[10] H. Latorre-Ossa, J.-L. Gennisson, E. De Brosses, and M. Tanter, "Quantitative imaging of nonlinear shear modulus by combining static elastography and shear wave elastography," *IEEE transactions on ultrasonics, ferroelectrics, and frequency control*, vol. 59, no. 4, pp. 833–839, 2012.

[11] C. F. Oteşteanu, B. R. Chintada, S. J. Sanabria, M. Rominger, E. Mazza, and O. Goksel, "Quantification of nonlinear elastic constants using polynomials in quasi-incompressible soft solids," in *Ultrasonics Symposium (IUS), 2017 IEEE International*. IEEE, 2017, pp. 1–4.

[12] S. Aristizabal, C. A. Carrascal, I. Z. Nenadic, J. F. Greenleaf, and M. W. Urban, "Application of acoustoelasticity to evaluate nonlinear modulus in ex vivo kidneys," *IEEE Trans Ultrasonics, Ferroelectrics, and Frequency Control*, vol. 65, no. 2, pp. 188–200, 2018.

[13] Y. Jiang, G.-Y. Li, L.-X. Qian, X.-D. Hu, D. Liu, S. Liang, and Y. Cao, "Characterization of the nonlinear elastic properties of soft tissues using the supersonic shear imaging (ssi) technique: inverse method, ex vivo and in vivo experiments," *Medical image analysis*, vol. 20, no. 1, pp. 97–111, 2015.

[14] C. F. Oteşteanu, B. R. Chintada, M. Rominger, S. Sanabria, and O. Goksel, "Spectral quantification of nonlinear elasticity using acousto-elasticity and shear-wave dispersion," *IEEE transactions on ultrasonics, ferroelectrics, and frequency control*, 2019.

[15] T. A. Krouskop, T. M. Wheeler, F. Kallel, B. S. Garra, and T. Hall, "Elastic moduli of breast and prostate tissues under compression," *Ultrasonic Imaging*, vol. 20, no. 4, pp. 260–274, 1998.

[16] J. Bercoff, M. Tanter, and M. Fink, "Supersonic shear imaging: a new technique for soft tissue elasticity mapping," *IEEE Trans Ultrasonics, Ferroelectrics, and Frequency Control*, vol. 51, no. 4, pp. 396–409, 2004.

[17] T. Loupas, J. Powers, and R. W. Gill, "An axial velocity estimator for ultrasound blood flow imaging, based on a full evaluation of the doppler equation by means of a two-dimensional autocorrelation approach," *IEEE Trans Ultrasonics, Ferroelectrics, and Frequency Control*, vol. 42, no. 4, pp. 672–688, 1995.

[18] P. Song, A. Manduca, H. Zhao, M. W. Urban, J. F. Greenleaf, and S. Chen, "Fast shear compounding using robust 2-d shear wave speed calculation and multi-directional filtering," *Ultrasound in medicine & biology*, vol. 40, no. 6, pp. 1343–1355, 2014.